BMC Gastroenterology

RESEARCH

Open Access

7-hydroxycoumarin ameliorates ulcerative colitis in mice by inhibiting the MAPK pathway and alleviating gut microbiota dysbiosis

Mengqi Liu[1*†], Huayi Sun[1†], Hao Fu[1], Lingping Fu[1], Xiao Zheng[1] and Yu Chen[1]

Abstract

Objective This research aimed to delineate the pharmacological mechanisms of 7-Hydroxycoumarin (7-HC) on ulcerative colitis (UC) employing network pharmacology and experimental validation.

Methods To investigate the therapeutic effects of 7-HC on UC, a UC mouse model was established through the unrestricted intake of 3.0% dextran sulfate sodium (DSS) in their drinking water. Subsequently, we predicted the core targets and signaling pathways of 7-HC for the treatment of UC using the network pharmacology approach. Finally, the insights gained from network pharmacology were further validated by molecular docking, molecular dynamics simulation as well as in vivo experiments.

Results Administering 7-HC orally to mice with UC led to a marked improvement in colitis indicators. Furthermore, 7-HC significantly lowered the levels of inflammatory cytokines (TNF-α, IL-1β) in the colon and modulated oxidative stress markers (MPO, SOD). Subsequent studies identified 2 core targets (AKT1 and EGFR) in the colon of UC mice that were inhibited by 7-HC. Network pharmacology and experimental validation showed that 7-HC can reduce the expression of MAPK pathway markers P38, JNK, ERK, and their phosphorylation; 7-HC can also ameliorate UC by regulating the gut microbiome.

Conclusion 7-HC demonstrates considerable efficacy in alleviating UC in mice, primarily through substantial diminution of tissue inflammation and oxidative stress. This is the first time that 7-HC has been found to treat UC by inhibiting the MAPK pathway and modulating the gut microbiota, providing a fresh perspective on the pharmacological mechanisms through which 7-HC operates in the management of UC.

Keywords 7-hydroxycoumarin, Ulcerative colitis, Network pharmacology, MAPK signaling pathway, Gut microbiome

†Mengqi Liu and Huayi Sun contributed equally to this work.

*Correspondence:
Mengqi Liu
1811040404@stu.hrbust.edu.cn
[1]Pharmacy College, Chengdu University of Traditional Chinese Medicine, Chengdu, China

Introduction

Ulcerative colitis (UC) is acknowledged within the medical community as a challenging disease to manage, primarily due to its recurrent and prolonged nature, which significantly impacts the work and quality of life of patients. Currently, there is an absence of specific medications for UC [1, 2]. Consequently, the development of efficacious treatments for UC represents a critical issue that demands immediate attention [3].

7-HC also referred to as umbelliferone, is prevalent in Chinese medicinal herbs and various vegetables [4]. Its significant pharmacological and biological properties have garnered increasing interest in the realms of functional foods and pharmaceuticals [5–9]. 7-HC has antitumor effects on colon cancer [7]. Importantly, recent studies suggest the potential therapeutic benefits of 7-HC in treating UC [3, 10]. However, the mechanism underlying 7-HC efficacy in UC treatment remains unexplored. Network pharmacology, an innovative methodology that combines systems biology with bioinformatics, offers valuable insights into the intricate mechanisms of drug actions [11], providing a solid theoretical foundation for future research in natural medicine. Therefore, network pharmacology was used to predict the mechanisms of 7-HC for treating UC, obtaining important targets and pathways. Finally, it was validated by in vitro experiments and biological techniques.

Materials and methods

7-HC 's therapeutic benefits in UC mice caused by DSS

SPF (Beijing) Biotechnology Co., Ltd., based in Beijing, China, provided thirty healthy male ICR mice, aged between 6 and 8 weeks. The Medical and Experimental Animal Ethics Committee of the CDUTCM granted ethical approval for these experiments under Ethics Approval No. SYXK2020-124, ensuring compliance with established ethical standards.

The research design included five experimental groups, each comprising six ICR mice. The grouping was as follows: a Control group, a DSS group, and three groups treated with 7-Hydroxycoumarin (7-HC) at dosages of 25 mg/kg (L-7-HC), 50 mg/kg (M-7-HC), and 100 mg/kg (H-7-HC), respectively [12]. 7-HC, with a purity greater than 98%, was procured from Chengdu Aiboke Biotechnology Co., LTD., Chengdu, China. To induce UC in mice, the mice were administered a 3.0% w/v dextran sulfate sodium (DSS) solution (No. 20230907, Seebio, Shanghai, China) from day 1 to day 7. Concurrently, from day 1 to day 10, 7-HC was orally administered to the designated groups, with the control group receiving a saline solution. The severity of colitis was monitored and quantified daily using the Disease Activity Index (DAI) [13]. After referring to The ARRIVE guidelines 2. 0 (https://arriveguidelines.org/arrive-guidelines), the method of choice for sacrifice of mice in this study was cervical dislocation. Cervical dislocation is a rapid and painless method of euthanasia in mice. The cervical vertebrae of the mouse are usually twisted rapidly by hand or tool, resulting in spinal cord injury, which causes immediate unconsciousness and cessation of respiration, and this method is only applicable to rodents weighing < 200 g. The mice selected in this study weighed an average of 30 g each and were eligible for the cervical dislocation method, in addition to being eligible for humanitarian execution of animals.

Histological examination

After the study, the colons were meticulously collected, dissected, and thoroughly examined. Following this, segments from each colon were immersed in a 4% (w/v) paraformaldehyde solution to achieve adequate fixation and stained using Hematoxylin and Eosin (H&E).

Enzyme-linked immunosorbent assays (ELISAs)

The concentrations of tumor necrosis factor-alpha (TNF-α, Catalog No. 20230925), interleukin-1β (IL-1β, Catalog No. 20230923), myeloperoxidase (MPO, Catalog No. 20230926), superoxide dismutase (SOD, Catalog No. 20230925), epidermal growth factor receptor (EGFR, Catalog No. 20240123), and RAC-alpha serine/threonine-protein kinase 1 (AKT1, Catalog No. 202401125) in colon tissues were determined using ELISA kits supplied by HeFei BoMei Biotechnology Co., Ltd., Hefei, China.

Cell viability assay

Briefly, 96-well plates were seeded with RAW264.7 cells and then treated with samples for 48 h. MTT solution (100 μL) was added to individual wells and left for 4 h. Afterward, each well received 150 μL of DMSO for 10 min. A microplate reader was employed to measure the optical density (OD) at 570 nm and compute each cell's survival rate.

Network pharmacology

To uncover the potential target genes of 7-HC, we utilized the SwissTarget Prediction database and subsequently aligned these targets with the UniProt database for verification and annotation. For the identification of UC-related target genes, the GeneCards and OMIM databases served as our primary resources. An analysis was conducted to find the overlap between the target genes of 7-HC and those associated with UC, pinpointing candidate therapeutic targets. The protein-protein interaction (PPI) networks were created from therapeutic targets by Cytoscape software for core therapeutic targets. For an in-depth understanding of the biological significance and pathways associated with these core targets,

KEGG and GO enrichment analyses were conducted using DAVID 6.8 (FDR <0.01).

Molecular docking

Network pharmacology studies frequently incorporate molecular docking as a validation tool. In this context, molecular docking analyses, conducted with AutoDock Vina, were utilized to verify the predicted interactions between 7-HC and its target proteins. Crystal structures of the AKT1, EGFR, and PKT2 were downloaded from the RCSB protein database and prepared using AutoDock Tools. The binding free energy (expressed in kcal/mol) was computed using the AutoDock Vina.

Quantitative real-time reverse transcription-polymerase chain reaction (qRT-PCR) analysis

RNA was extracted from colon tissues utilizing RNA extraction reagents. Following the extraction, the HiFiScript gDNA Removal cDNA Synthesis Kit was employed to synthesize cDNA, which was subsequently stored at -20 °C for qRT-PCR analyses. The assessment of EGFR and AKT1 expression levels was carried out in a 20 μL reaction volume, as specified in Primer Table 1. For qPCR analysis, SYBR Green qPCR Master Mix (with High Rox) was used, adhering to the supplied protocols, with 2 μL of cDNA utilized per sample within a three-step amplification process on a Bio-Rad real-time PCR detector. Each sample was tested in triplicate, employing GAPDH as the normalization control, providing a quantitative measure of EGFR and AKT1 gene expression in the colon tissue samples.

Molecular dynamics simulation (MDS)

The MDS of 7-HC and AKT1 were performed using the GROMACS 5.1.4 software package to validate the molecular docking results. Determining the binding shape and energy between the ligand and receptor was the aim of these simulations. Energy minimization was done first, using the molecular docking results (7-HC and AKT1) as the starting configuration. MDS running in a vacuum for 500 ps were then performed,. Afterward, the isothermal-isobaric ensemble (NPT) and the canonical ensemble (NVT) were both used to equilibrate the system. Ultimately, the molecular dynamics simulations were run at ambient temperature and pressure for 30 ns.

Table 1 Primer sequences

Gene	Primer sequence (5′ – 3′) Forward primer	Reverse primer
EGFR	TGACTGTCTGGTCTGCCAAAAG	ATGCCATCTTCT TCCACTTCGT
AKT1	GCTGCTCAAGAAGGACCCTAC	GCTTCTTCTCAT ACACATCCTGC
GAPDH	CCTCGTCCCGTAGACAAAATG	TGAGGTCAATG AAGGGGTCGT

Western blot

Western blotting was the chosen method to evaluate the protein expression levels of MAPK pathway-related proteins, including phosphorylated p38 (p-p38), p38, C-Jun N-terminal kinase (JNK), p-JNK, extracellular signal-regulated kinase (ERK), and p-ERK within colon tissues from the various experimental groups. The process began with homogenizing the colon tissues, followed by centrifugation to separate the supernatant. The protein concentrations in these samples were then quantified to standardize the amount of protein loaded onto gels. Subsequent steps involved subjecting the samples to SDS-PAGE electrophoresis, transferring the separated proteins onto membranes, and blocking nonspecific binding sites. The membranes were then incubated with specific primary antibodies against six MAPK pathway-related proteins (all diluted at 1:1000, sourced from Protein-tech Group, Inc., Wuhan, China), as well as with ACTIN (diluted at 1:2000) serving as the loading control. The detection of protein bands was achieved through enhanced chemiluminescence (ECL), with ImageJ software being utilized to quantify the intensity of these bands, allowing for the precise measurement of protein expression levels in the colon tissues.

Gut microbiota analysis by 16 S rRNA gene sequencing

PANOMIX Biomedical Tech Co., Ltd (Suzhou, China) performed 16 S rRNA sequencing using the following method: fecal samples were harvested as used to extract total DNA, the quality of which was then assessed via 1.2% agarose gel electrophoresis. Specific primers were then utilized to amplify the V3-V4 region of the 16 S rRNA gene via PCR, after which a TruSeq Nano DNA LT Library Prep Kit from Illumina was used for library preparation, followed by sequencing which was performed with the Illumina MiSeq-PE250 platform (Illumina, USA). Operational taxonomic unit (OTU) assignments were made at a 97% sequence similarity threshold. QIIME2 was used to analyze alpha and beta diversity. Significant differences in microbial taxa abundance among treatment groups were evaluated with a linear discriminant analysis effect size (Lefse) approach.

Statistical analysis

Data were analyzed using SPSS software, version 26.0. The results are expressed as means±standard deviation (SD). For comparative analysis among the groups, analysis of variance (ANOVA) was employed, followed by either LSD or Dunnett's T3 post hoc tests, depending on the data distribution and variance homogeneity. Statistical significance was established at a P-value of less than 0.05.

Results

7-HC significantly improves colonic injury in UC mice

Figure 1A depicts the methodology for drug administration and animal modeling. Mice in the DSS-induced colitis group displayed characteristic UC symptoms such as reduced body weight, spleen enlargement, and significant reduction in colon length. These variations were statistically significant ($P<0.001$), as presented in Fig. 1B and E. However, treatment with 7-HC ameliorated these changes, with the effects of high-dose 7-HC (H-7-HC) being particularly notable. Histological analysis via H&E staining revealed that DSS administration caused marked damage to the colonic crypts and epithelial cells. Conversely, 7-HC treatment effectively mitigated this damage, as illustrated in Fig. 1F.

7-HC alleviates UC mice by being anti-inflammatory and antioxidant

Treatment with DSS resulted in elevated levels of IL-1β and TNF-α within the colon tissues (Fig. 2A and B). Treatment with 7-HC mitigated these increases to various degrees, with the high dosage of 7-HC (H-7-HC)

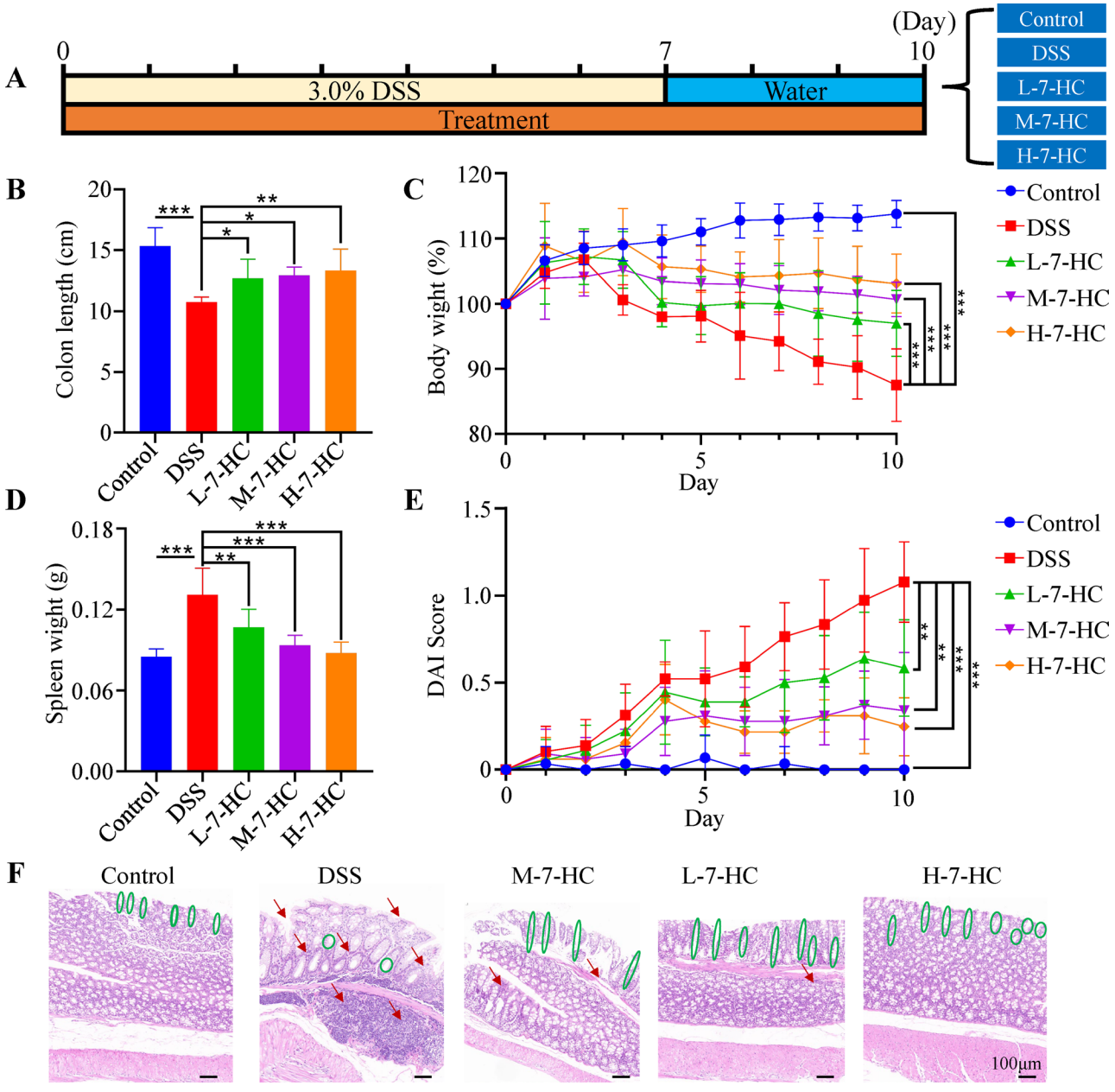

Fig. 1 7-HC attenuated DSS-induced colitis in mice. (**A**) Treatment and modeling cycle. (**B**) Histogram showing the evaluation of colon lengths. (**C**) Mouse body weights. (**D**) Histogram showing the evaluation of spleen weights. (**E**) DAI graph scores as a function of time. (**F**) H&E staining of colonic sections. Data are mean ± SD, $n=6$. *$P<0.05$, **$P<0.01$, ***$P<0.001$

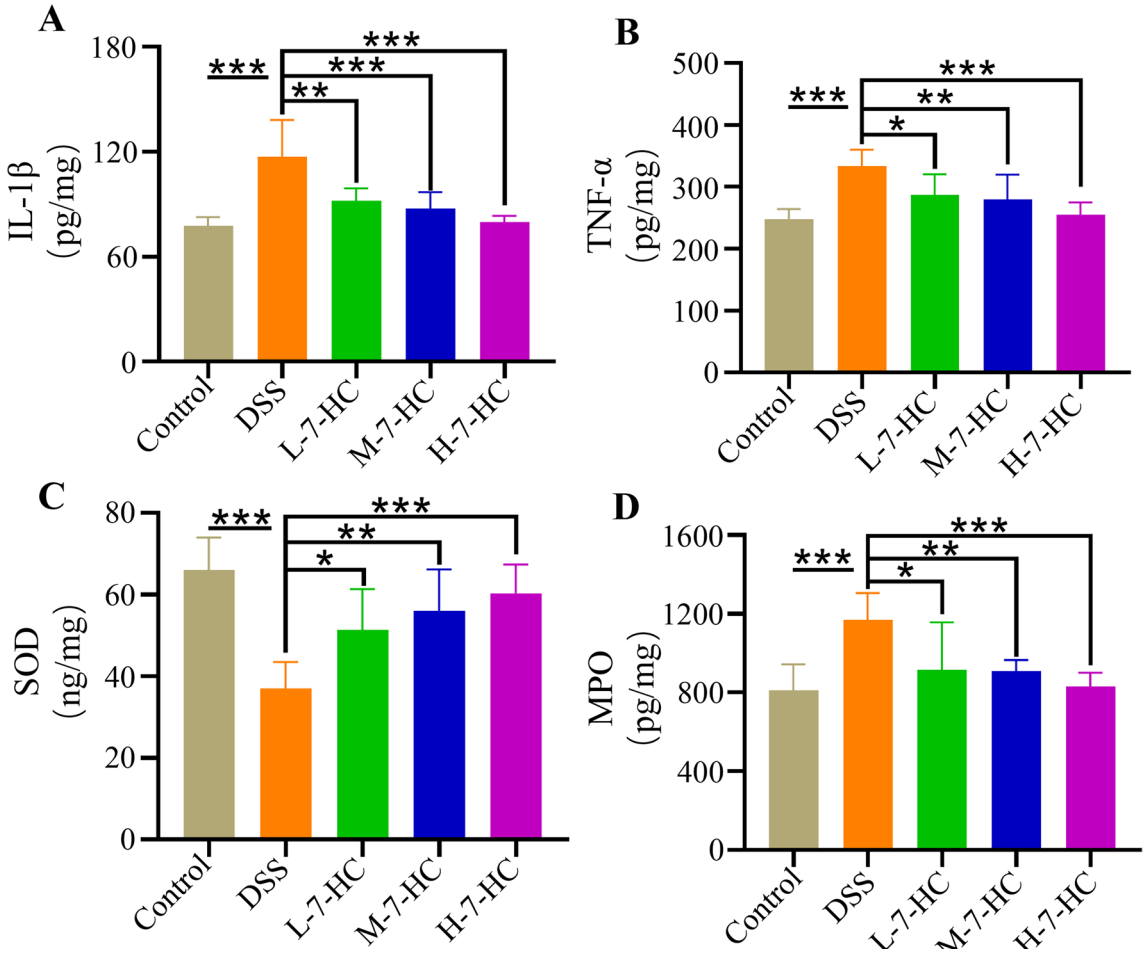

Fig. 2 7-HC alleviates UC mice by being anti-inflammatory and antioxidant. Histogram showing changes in the levels of IL-1β (**A**), TNF-α (**B**), SOD (**C**), and MPO (**D**) in the colon after different doses of 7-HC. Data are mean ± SD, $n = 6$. *$P < 0.05$, **$P < 0.01$, ***$P < 0.001$

demonstrating the most significant reduction in the concentrations of the pro-inflammatory cytokines IL-1β and TNF-α, compared to medium (M-7-HC) and low (L-7-HC) dosages. Inflammatory conditions are frequently associated with oxidative stress. Therefore, to explore the influence of 7-HC on oxidative stress in UC-afflicted mice, superoxide dismutase (SOD) and myeloperoxidase (MPO) activities in colon tissues were assessed. The data, as illustrated in Fig. 2C and D, revealed that 7-HC administration significantly enhanced SOD activity and concurrently reduced MPO activity, indicating a decrease in oxidative stress compared to the DSS-treated group. Notably, the high dosage of 7-HC was particularly effective in elevating SOD activity and lowering MPO levels when contrasted with medium and low dosages.

7-HC had excellent biocompatibility

To evaluate the toxic and side effects of 7-HC, MTT assay was determined. According to the MTT assay results (Figure S1), 7-HC (20–80 μM) did not significantly harm RAW264.7 macrophages, which exhibited viabilities of 85% over a 48 h incubation period.

Mechanisms prediction of 7-HC for treating UC based on network pharmacology

Identification of UC-related therapeutic targets and core targets

A total of 64 target genes related to 7-HC were identified, alongside 6470 target genes associated with UC, derived from existing databases. An intersection of these two gene sets revealed 39 potential therapeutic target genes (Fig. 3A). Subsequently, PPI network comprising these target genes (Fig. 3B), which encompassed 38 nodes (target proteins) and 288 edges (interactions between proteins). Moreover, three core targets were identified, each with degree values exceeding the average (15.16), namely AKT1, EGFR, and PKT2. These targets may play pivotal roles in the 7-HC-mediated therapeutic approach for UC.

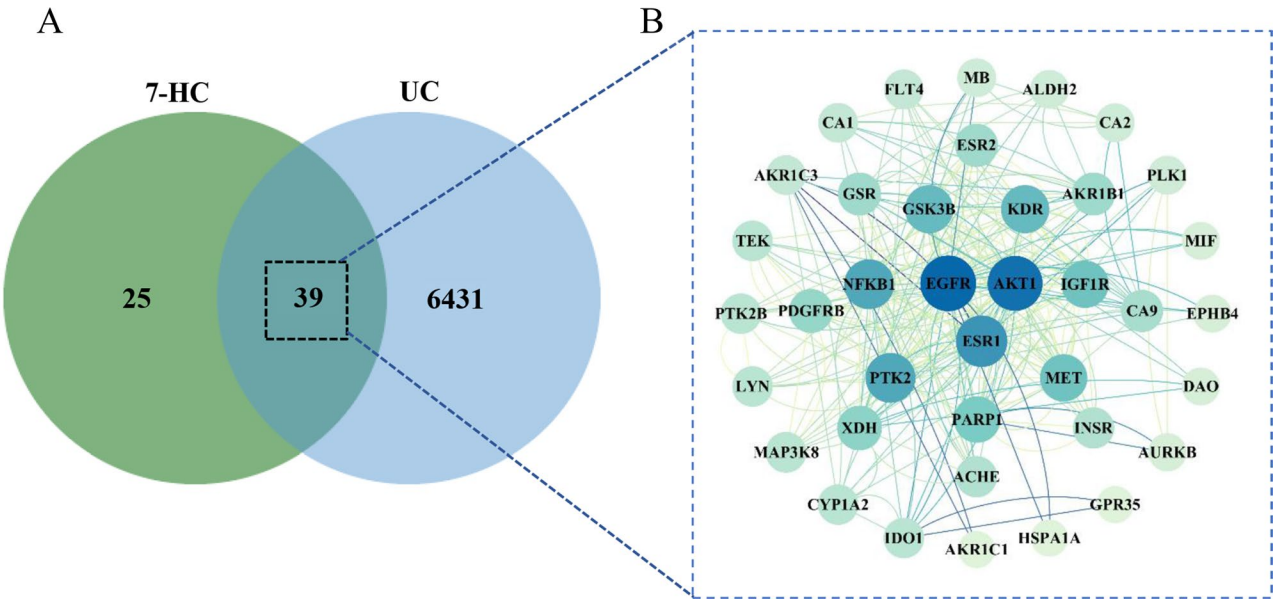

Fig. 3 Identification of 39 potential therapeutic targets (**A**). PPI network of the 39 potential therapeutic targets with identification of 3 core targets (**B**)

GO and KEGG enrichment analysis

The elucidation of 7-HC's mechanisms in treating ulcerative colitis (UC) was advanced through GO and KEGG analyses performed on 39 identified therapeutic targets. The GO analysis revealed 109 significant categories ($P<0.01$), illustrated in Fig. 4A-C, with a predominant focus on Biological Processes (BP), which included 65 categories. These processes mainly pertained to the negative regulation of the apoptotic process, protein autophosphorylation, and signal transduction. Cellular Components (CC) comprised 13 categories, with emphasis on the cytosol, plasma membrane, and cytoplasm. Molecular Function (MF) was highlighted across 30 categories, primarily relating to protein and ATP binding.

The KEGG pathway enrichment analysis uncovered 38 pathways, with the most significant 15 depicted in Fig. 4D. These pathways largely converge on inflammation and various diseases, underscoring inflammation-related pathways like the PI3K-Akt and MAPK pathways, as well as disease-specific pathways such as those associated with Prostate and Breast cancer. This suggests that 7-HC's therapeutic action against UC may operate through modulating both inflammation and disease-associated pathways, offering insights into the comprehensive biological impact of 7-HC in the context of UC treatment.

Mechanism verification of 7-HC therapy for UC

Molecular docking of 7-HC and core targets

To corroborate the PPI network findings, molecular docking was conducted to examine three core targets. The docking results indicate that 7-HC can bind to core targets such as AKT1 (-7.3), EGFR (-6.6), and PKT2 (-5.8), suggesting its potential role in mitigating UC.

ELISA and qRT-PCR of core targets

The top 2 core targets (AKT1 and EGFR) in the molecular docking results were selected for experimental validation. To further validate these core targets, enzyme-linked immunosorbent assays (ELISAs) were performed (Fig. 5A **and B**), which demonstrated significant elevations in AKT1 and EGFR levels in UC mouse models compared to controls ($P<0.001$). Additionally, 7-HC was shown to counteract the downregulation of these proteins in a dose-dependent manner. Similarly, qRT-PCR analyses showed the same results (Fig. 5C). These findings provide substantive evidence of 7-HC's capability to modulate these core targets, contributing to its efficacy in treating UC.

Molecular dynamic simulation

Among the molecular docking results, 7-HC demonstrated the highest binding affinity with AKT1. To further verify 7-HC's binding capability with AKT1, a molecular dynamics simulation was conducted. Root-mean-square deviation (RMSD) curves showed fluctuations in the protein's conformation (Fig. 6A), indicating that after 10 ns, the 7-HC-AKT1 complex stabilized, suggesting minimal changes in AKT1's conformation post-binding with 7-HC and thus, the interaction is relatively stable. The absence of breaks in the RMSD curve suggests that 7-HC remains firmly bound to AKT1 throughout the simulation, without detaching from the protein pocket. The number of hydrogen bonds within the AKT1-7-HC complex reflects the binding strength, with 7-HC-AKT1

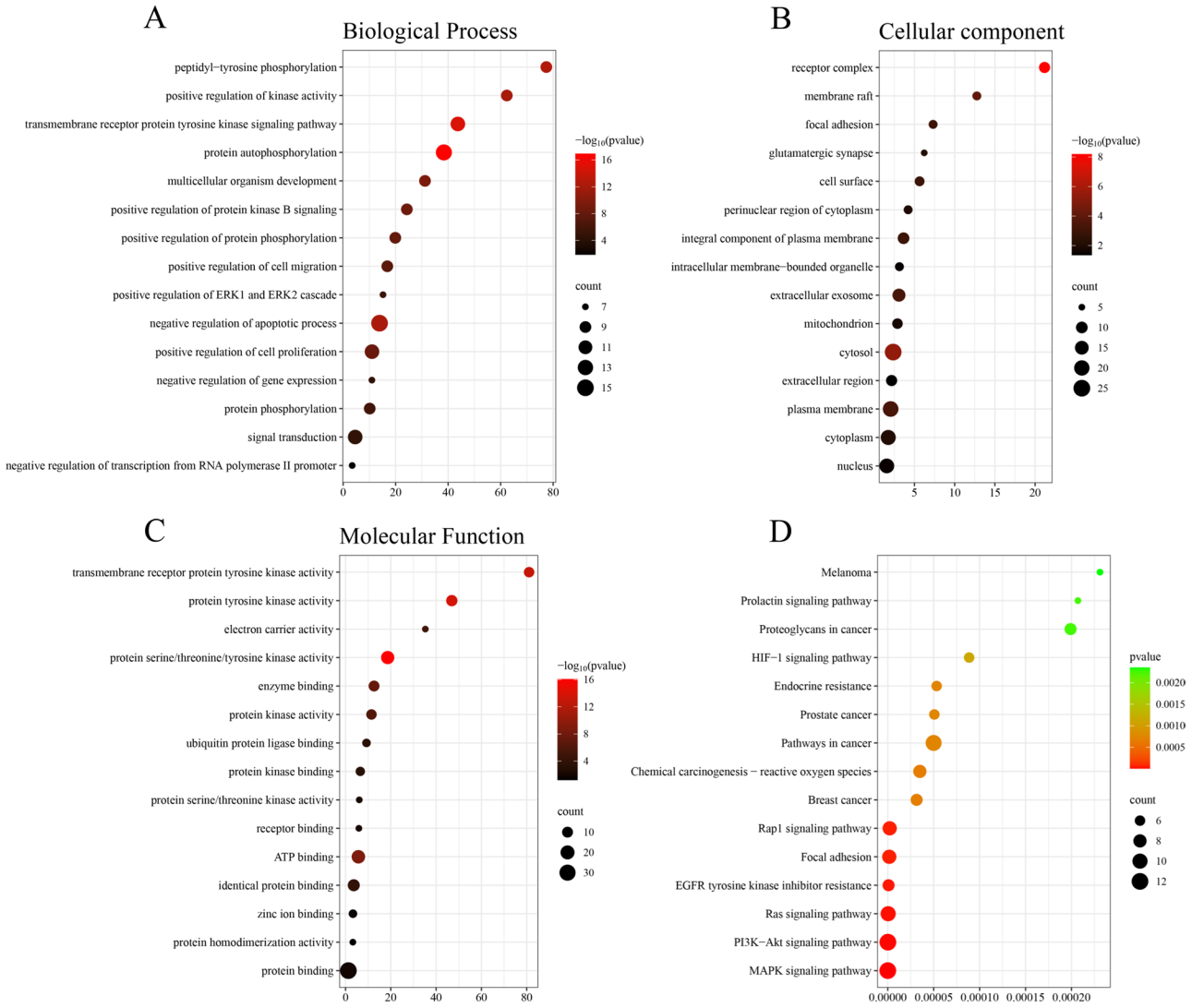

Fig. 4 The bubble plots for GO and KEGG pathway enrichment analysis. (**A**) The bubble plots for BP. (**B**) The bubble plots for CC. (**C**) The bubble plots for MF. (**D**) The bubble plots for KEGG pathway enrichment

exhibiting the highest density and strength of hydrogen bonds, as depicted in Fig. 6B. Furthermore, the radius of the gyration curve, indicating the compactness of the protein structure, showed that 7-HC-AKT1 maintains stable radii of gyration, corroborated by RMSD results, which implies that the protein structure remains stable (Fig. 6C). Additionally, the solvent-accessible surface area (SASA) of the 7-HC-AKT1 complex showed a gradual decrease, suggesting an increase in the binding interaction over time (Fig. 6D).

7-HC alleviates UC mice by inhibiting MAPK signaling pathway

Further examination focused on the expression levels of crucial proteins within the MAPK pathway. The results from Western blot analysis, as depicted in Fig. 7A and B, demonstrated that the administration of DSS led to an increase in the expression levels of ERK, JNK, p38, as well as their phosphorylated forms (p-ERK, p-JNK, and p-p38). Conversely, treatment with 7-HC notably decreased the expression of these proteins, suggesting a significant reduction in MAPK pathway activity. These observations indicate that 7-HC exerts its therapeutic effects on UC in mice primarily through the inhibition of the MAPK pathway.

7-HC alleviates UC mice via the remodeling of the gut microbiome

A Venn diagram revealed that 7-HC treatment was associated with an increase in OTU counts that were shared with those of control mice, suggesting some degree of similarity with respect to the species composition in the gut of 7-HC -treated and control mice (Fig. 8A). α-diversity analyses of species diversity and richness were

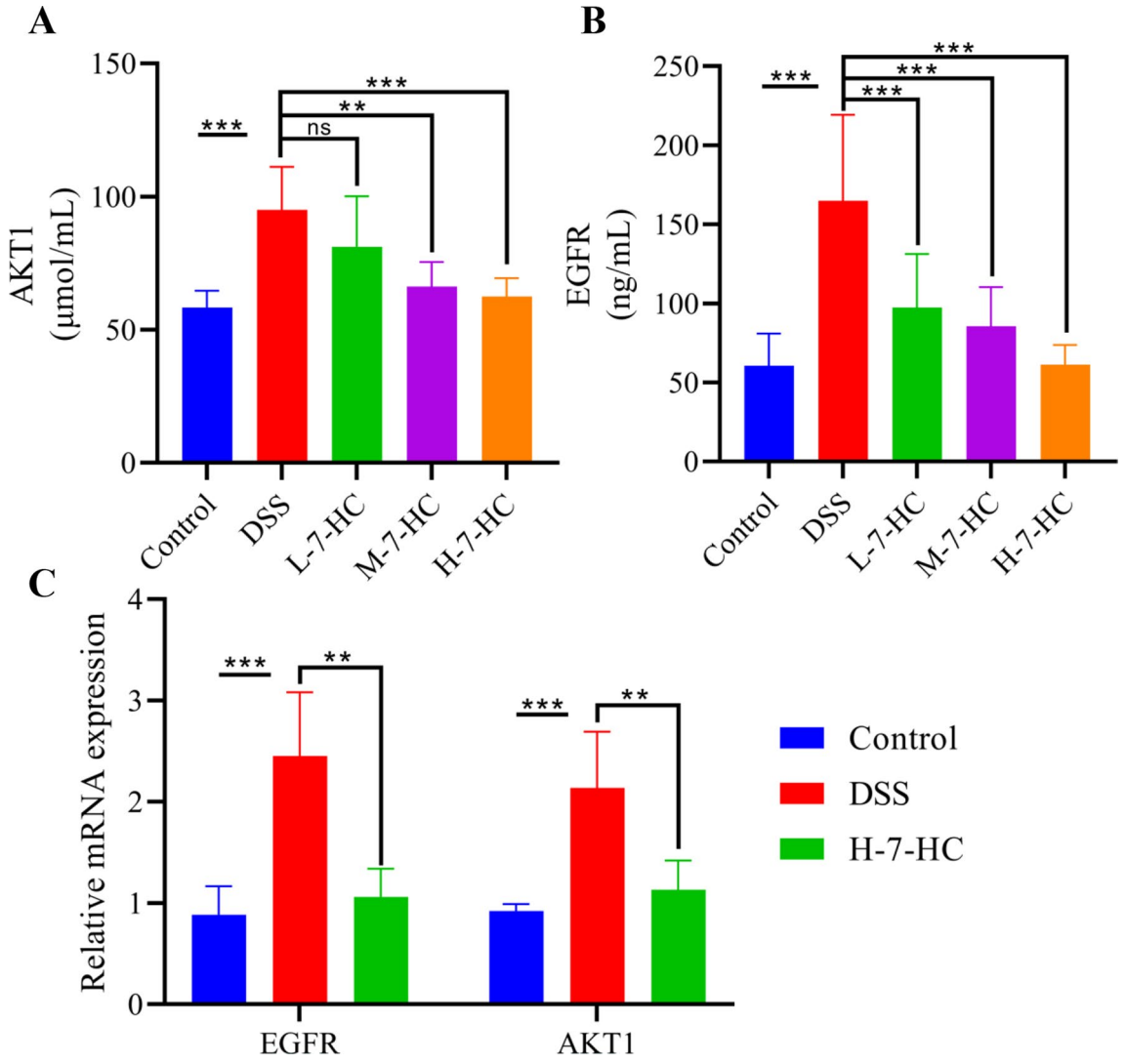

Fig. 5 Verification of 3 core targets. (**A**-**B**) Histogram showing changes in the levels of EGFR and AKT1 in the colon after different doses of 7-HC ($n=6$). (**C**) RT-PCR analysis of the mRNA levels of EGFR and AKT1 ($n=4$). Data are mean ± SD. *$P<0.05$, **$P<0.01$, ***$P<0.001$

also conducted using these samples, revealing that 7-HC administration was associated with marked increases in microbial abundance and diversity in these UC model mice as evidenced by the Observed_species, Chao1, and Shannon indices (Fig. 8B and D). β-diversity (PCoA and NMDS) approaches were then used to assess similarity among microbial communities (Fig. 8E and F). This strategy revealed that the gut microbiota in DSS-treated model mice was substantially different from that of control mice, whereas 7-HC abrogated these DSS-related changes.

To further elucidate the effects of 7-HC on the composition of the gut microbiota, changes in gut microbiota composition at the phylum, family, and genus levels were compared among different groups. At the phylum level, 7-HC reduced relative abundance of Verrucomicrobia and Actinomycetota while increasing the relative abundance of Bacillota and Pseudomonadota in UC mice (Fig. 8G). 7-HC reduced relative *Erysipelotrichaceae* and *Tannerellaceae* abundance at the family level while increasing relative *Lactobacillaceae* and *Clostridiaceae* abundance in UC mice (Fig. 8H). At the genus level, 7-HC reduced relative *Faecalibaculum* and *Porphyromonas* abundance while increasing relative *Lactobacillus* and *Hungatella* abundance in uc mice (Fig. 8I). Overall, these results suggest that the administration of 7-HC can modulate the composition of the gut microflora in UC mice.

Discussion

In this study, oral administration of 7-HC to mice with UC models significantly mitigated colitis symptoms, and reduced levels of colonic inflammatory cytokines as well as oxidative stress markers. Subsequently,

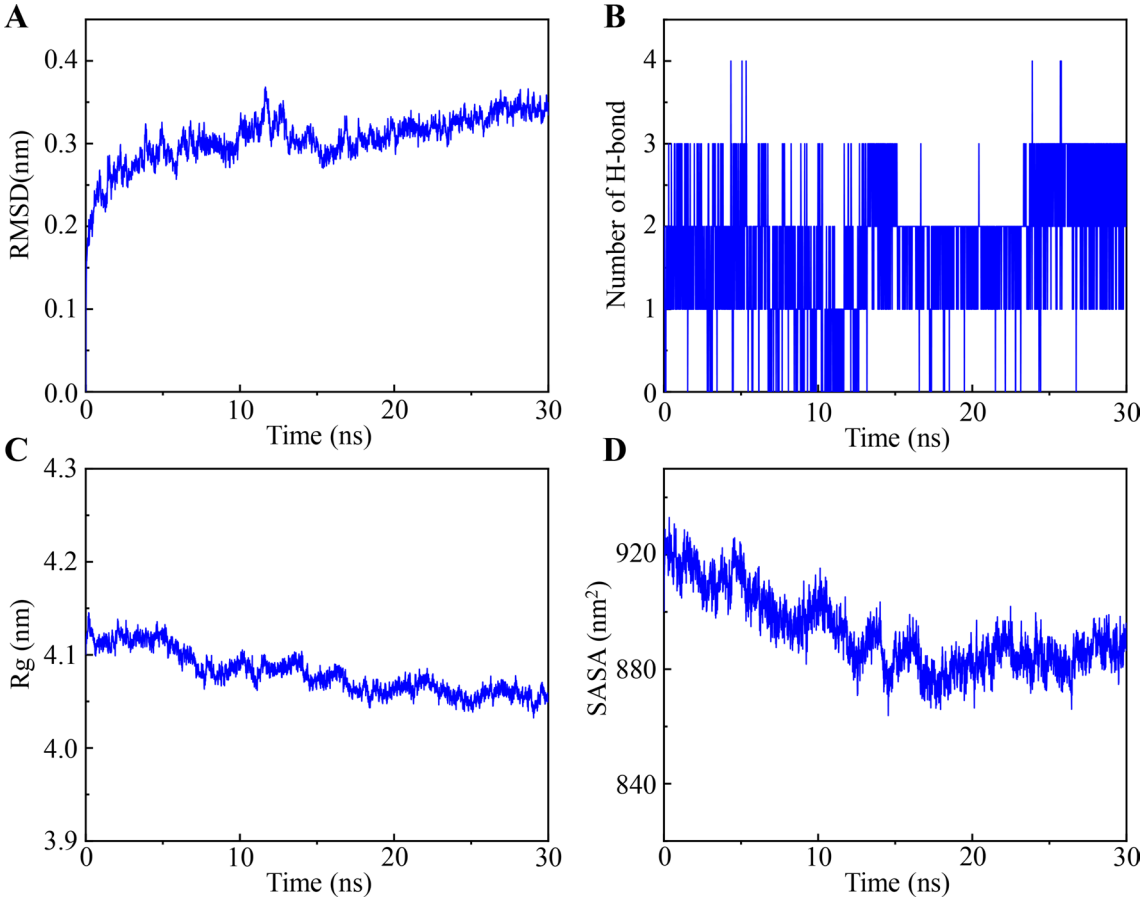

Fig. 6 Molecular dynamic simulation. (**A**) Root mean square fluctuation (RMSD) values extracted from the protein-fit ligand of the protein-ligand docked complexes. (**B**) H bond formation between 7-HC and AKT1. (**C**) The compactness of the protein structure in terms of the radius of gyration (Rg). (**D**) Solvent accessible surface area (SASA) analysis

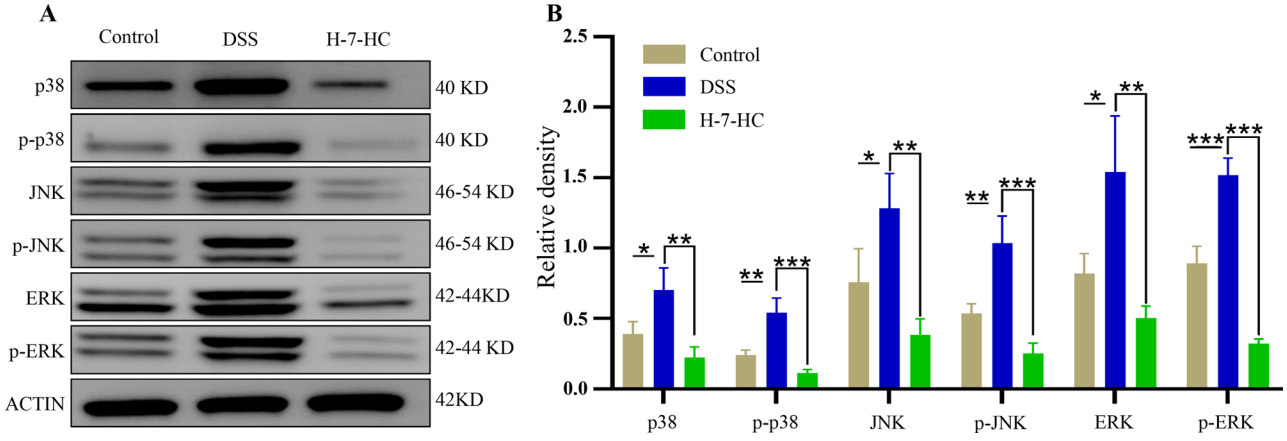

Fig. 7 7-Hydroxycoumarin inhibited MAPK signaling pathways. (**A**) Western blotting of ERK, JNK, p38, p-ERK, p-JNK, and p-p38. (**B**) Quantification of ERK, JNK, p38, p-ERK, p-JNK, and p-p38 protein levels by ImageJ software ($n = 3$). Data are mean ± SD. *$P < 0.05$, **$P < 0.01$, ***$P < 0.001$

network pharmacology identified 39 potential therapeutic targets for 7-HC in UC treatment, indicating that 7-HC may act on multiple targets to exert its anti-UC effects. KEGG analysis revealed that these targets are predominantly involved in inflammatory pathways, including the MAPK and PI3K-AKT pathways. Screening of the PPI network pinpointed 3 core targets (AKT1, EGFR, PKT2) for 7-HC's action in UC. Molecular docking, dynamics simulation results, qRT-PCR, and ELISA confirmed that 7-HC could bind to these

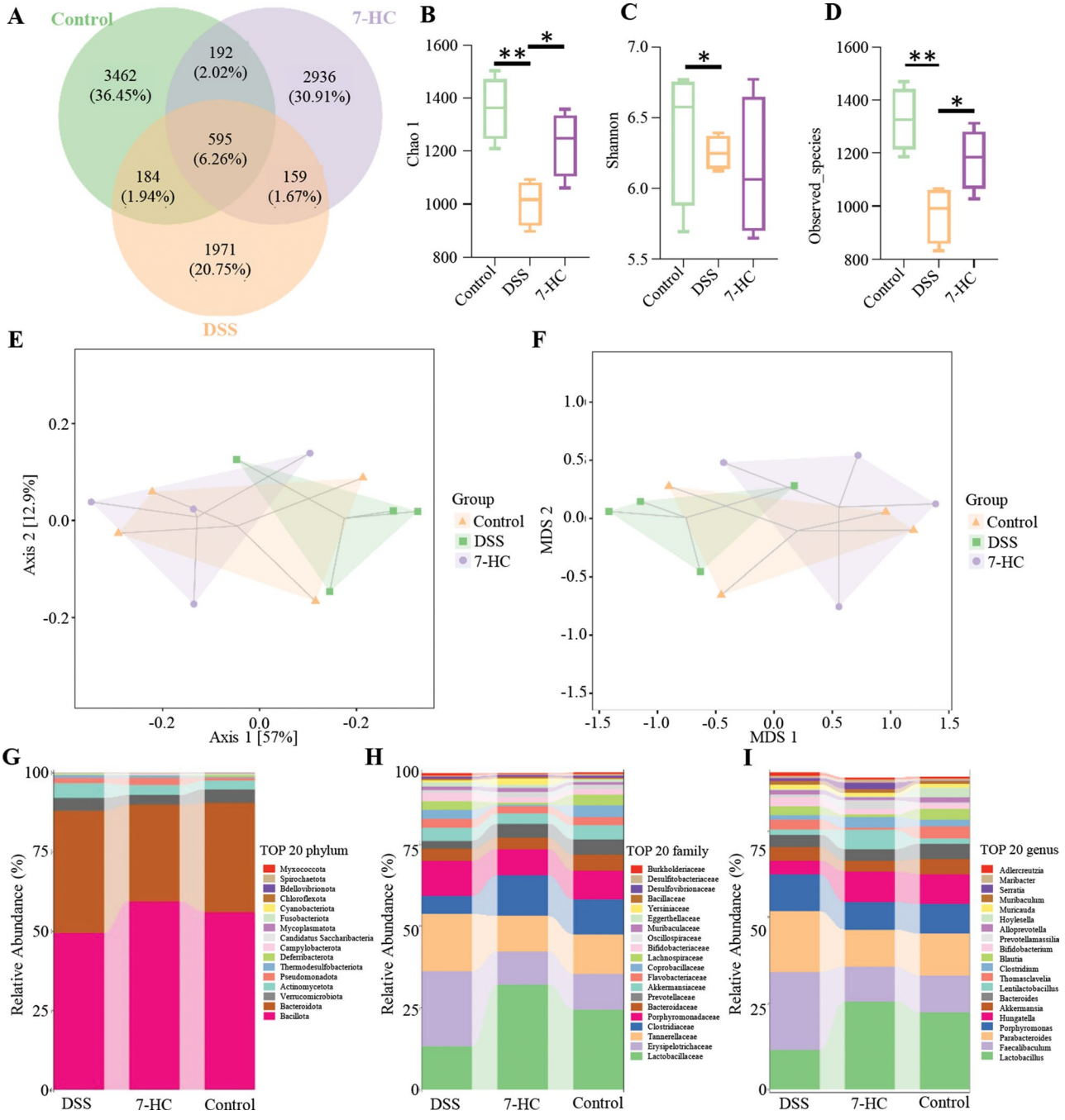

Fig. 8 Effects of 7-Hydroxycoumarin on the diversity and community structures of gut microbiota in UC mice. (**A**) Wayne diagram showing common and unique OTUs between the groups. (**B**) Chao1 index analysis. (**C**) Shannon index analysis. (**D**) Observed_species index analysis. (**E**) Principal coordinate analysis of gut microbiota based on weighted UniFrac distance; (**F**) NMDS analysis of gut microbiota based on the Bray-Curtis distance. (**G**) The relative abundance of gut microbiota in each group at the phylum level. (**H**) The relative abundance of gut microbiota in each group at the family level. (**I**) The relative abundance of gut microbiota in each group at the genus level. Data are mean ± SD, $n = 4$. $^{*}P < 0.05$, $^{**}P < 0.01$, $^{***}P < 0.001$

core targets, and Western blot analysis demonstrated that 7-HC effectively inhibits the MAPK signaling pathway (Fig. 9). In addition, the MAPK pathway is closely related to gut microbiome. Therefore, we also explored the effect of 7-HC on the gut microbiome.

It has been demonstrated that mitigating the expression of p38, JNK, and ERK within the MAPK pathway can suppress pro-inflammatory cytokines (IL-1β and TNF-α), thereby alleviating UC symptoms and macrophage-induced inflammation in mice [14–17]. Notably, this study found that 7-HC may exert

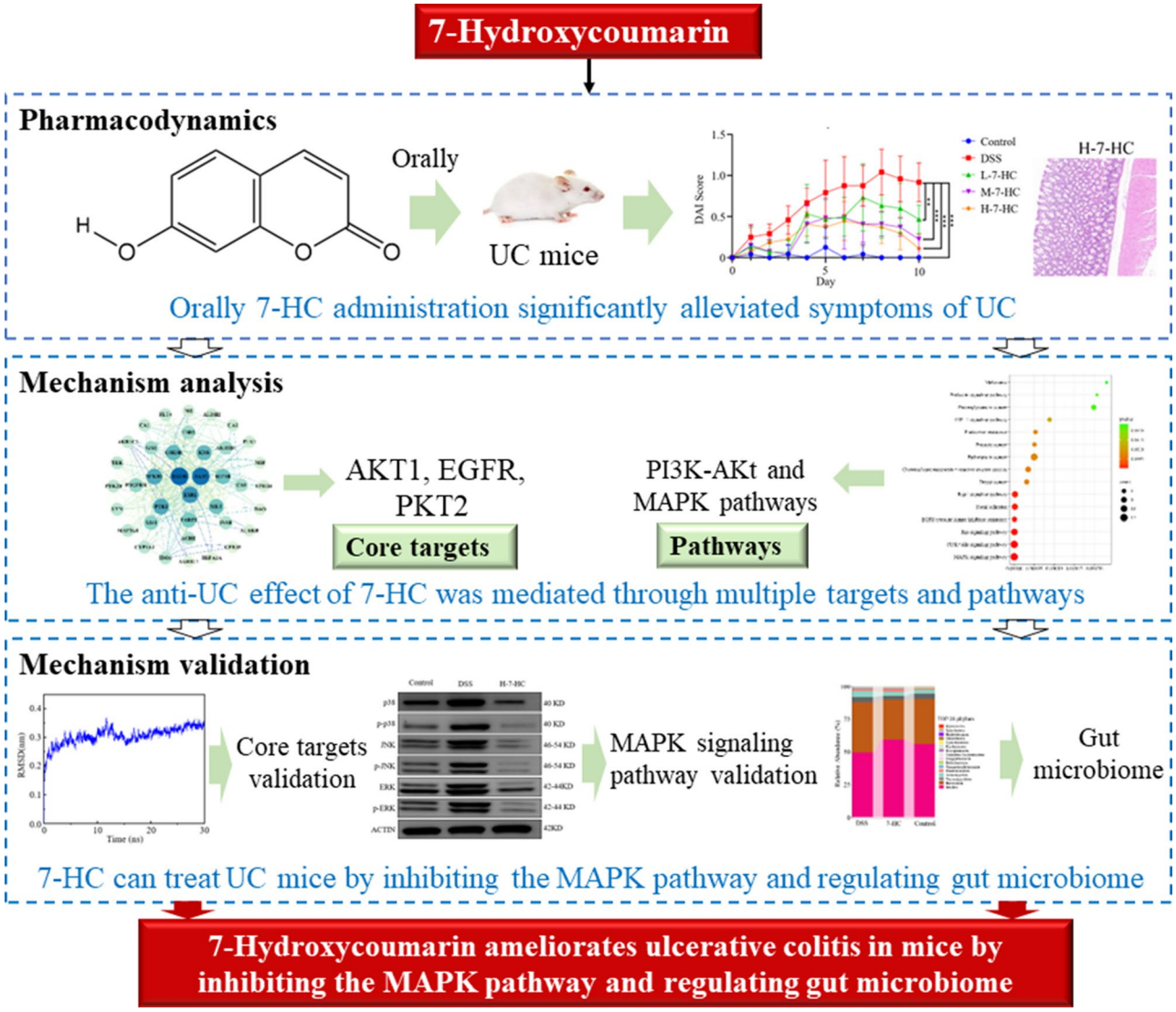

Fig. 9 7-Hydroxycoumarin ameliorates DSS-induced ulcerative colitis via the MAPK signaling pathway

anti-inflammatory effects and alleviate UC symptoms by inhibiting the MAPK pathway.

AKT1 is essential for acute inflammation, principally by regulating vascular permeability, which results in edema and the efflux of leukocytes [18]. Activation of AKT1 has been identified to enhance vascular permeability, contributing to the pathogenesis of DSS-induced UC [19]. On the other hand, the epidermal growth factor receptor (EGFR) is crucial for the proliferation, defense, and repair mechanisms of colonic mucosal epithelial cells [20]. Studies have demonstrated a significant increase in EGFR expression during the early stages of colonic inflammation in UC, underscoring its critical role in mucosal repair. However, overactivation of EGFR may lead to vascular dysregulation in the tissue and increase the risk of cancer [20]. Therefor, 7-HC could alleviate inflammation in colonic tissues of UC mice by inhibiting the expression of AKT1 and EGFR.

However, the present study has several limitations. Firstly, information from online databases is based on reviewed and predicted data; therefore, targets of 7-HC that are unproven and undocumented may not be included in our analysis. Secondly, further pharmacological experiments in vitro and in vivo are needed to validate the therapeutic mechanism of 7-HC on UC. Lastly, the anti-UC effect of 7-HC needs to be further verified in animal models and clinical trials.

Conclusion

In conclusion, this study demonstrates that 7-HC ameliorates inflammatory responses and oxidative stress in the colonic tissues of UC mice by inhibiting the MAPK pathway and modulating the gut microbiota.

In addition, the present study also demonstrated that 7-HC has great potential to target AKT1, EGFR, and PKT2 in UC mice. These findings offer a theoretical foundation and valuable insights for further pharmacological research and the clinical use of 7-HC in combating UC.

Abbreviations

DAI	Disease activity index
DSS	Dextran sodium sulfate
ELISA	Enzyme-linked immunosorbent assays
H&E	Hematoxylin and Eosin
MAKP	Mitogen-activated protein kinases
UC	Ulcerative colitis
TNF-α	Tumor necrosis factor-α

Supplementary Information

The online version contains supplementary material available at https://doi.org/10.1186/s12876-024-03499-y.

Supplementary Material 1

Supplementary Material 2

Acknowledgements
We would like to thank Mr. Huang You from Chengdu University of Traditional Chinese Medicine for his selfless guidance and selfless help with the experiments.

Author contributions
Mengqi Liu and Huayi Sun: Conceptualization, Writing–review & editing, Performed experiments, Data curation, and Writing–original draft. Lingping Fu, and Hao Fu: Performed experiments, Writing–review & editing, Formal analysis. Xiao Zheng, Yu Chen, and Mengxia Wu: Writing–review & editing and Formal analysis.

Funding
The work was supported in part by the grant of the scholarship (NO. EDJ2023-0901) from Chengdu University of Traditional Chinese Medicine.

Data availability
The datasets generated and analyzed during the current study are not publicly available due to potential commercial misuse but are available from the corresponding author on reasonable request.

Declarations

Ethics approval and consent to participate
The Medical and Experimental Animal Ethics Committee of the Chengdu University of Traditional Chinese Medicine granted ethical approval for these experiments under Ethics Approval No. SYXK2020-124, ensuring compliance with established ethical standards.

Consent for publication
Not applicable.

Competing interests
The authors declare no competing interests.

Conflict of interest
No conflicts of interest are associated with this publication.

Received: 6 July 2024 / Accepted: 7 November 2024
Published online: 12 November 2024

References

1. Eisenstein M. Ulcerative colitis: towards remission. Nature. 2018;563(S33). https://doi.org/10.1038/d41586-018-07276-2.
2. Ordás I, Eckmann L, Talamini M, et al. Ulcerative colitis. Lancet. 2012;380:1606–19. https://doi.org/10.1016/s0140-6736(23)00966-2.
3. Huang Y, Li S, Wu QH, et al. Study on the mechanism of action of seven compounds in the treatment of ulcerative colitis based on network pharmacology. Nat Prod Res Dev. 2023;35:662–76. https://doi.org/10.16333/j.1001-6880.2023.4.014.
4. Jesus RLC, Silva ILP, Araújo FA, et al. 7-Hydroxycoumarin induces vasorelaxation in animals with essential hypertension: focus on Potassium channels and intracellular ca(2+). Mobilization Molecules. 2022;27. https://doi.org/10.3390/molecules27217324.
5. Ru J, Li P, Wang J, et al. TCMSP: a database of systems pharmacology for drug discovery from herbal medicines. J Cheminf. 2014;6:13. https://doi.org/10.1186/1758-2946-6-13.
6. Vasconcelos JF, Teixeira MM, Barbosa-Filho JM, et al. Effects of umbelliferone in a murine model of allergic airway inflammation. Eur J Pharmacol. 2009;609:126–31. https://doi.org/10.1016/j.ejphar.2009.03.027.
7. Wu WF, Wang JN, Li Z, et al. 7-Hydroxycoumarin protects against cisplatin-induced acute kidney injury by inhibiting necroptosis and promoting Sox9-mediated tubular epithelial cell proliferation. Phytomedicine. 2020;69:153202. https://doi.org/10.1016/j.phymed.2020.153202.
8. Sami DH, Soliman AS, Khowailed AA, et al. 7-hydroxycoumarin modulates Nrf2/HO-1 and microRNA-34a/SIRT1 signaling and prevents cisplatin-induced oxidative stress, inflammation, and kidney injury in rats. Life Sci. 2022;310:121104. https://doi.org/10.1016/j.lfs.2022.121104.
9. Kabeya LM, Fuzissaki CN, Taleb SH, et al. 7-Hydroxycoumarin modulates the oxidative metabolism, degranulation and microbial killing of human neutrophils. Chem Biol Interact. 2013;206:63–75. https://doi.org/10.1016/j.cbi.2013.08.010.
10. Cruz LF, Figueiredo GF, Pedro LP, et al. Umbelliferone (7-hydroxycoumarin): a non-toxic antidiarrheal and antiulcerogenic coumarin. Biomed Pharmacother. 2020;129:110432doi. https://doi.org/10.1016/j.biopha.2020.110432.
11. Huang Y, Yang SS, Lin X, et al. Study on the mechanism of action of Fuzi Lizhong pills in treating ulcerative colitis based on network pharmacological-molecular docking. Chin J Pharm Sci. 2019;55:1812–22. https://doi.org/10.16438/j.0513-4870.2019-0936.
12. Wang J, Ishfaq M, Fan Q, et al. 7-Hydroxycoumarin attenuates Colistin-Induced kidney injury in mice through the decreased level of histone deacetylase 1 and the activation of Nrf2 signaling pathway. Front Pharmacol. 2020;11:1146doi. https://doi.org/10.3389/fphar.2020.01146.
13. Wang L, Liu Y, Shen G, et al. Mechanisms of Si-Wu Decoction in the treatment of ulcerative colitis revealed by network pharmacology and experimental verification. J Ethnopharmacol. 2023;317:116847. https://doi.org/10.1016/j.jep.2023.116847.
14. Tang M, Liu Q, Liu H, et al. Research progress of ulcerative colitis related signaling pathways. Chin Pharm Bull. 2018;34:1642–7.
15. Li ZH, Wang J, Cai RL. Effects of Shenling Baizhu powder on the expressions of AQP3 and AQP4 in UC rats via ERK/p38 MAPK signal pathway. Chin Tradit Pat Med. 2015;37:1883–8.
16. Chen S, He Y, Wu Q. The research on observing the effect of Baishaoqiwu granules acting mechanism in treating Ulcerative colitis from NOXs-ROS-P38MAPK related signal pathway. Lishizhen Med Mater Med Res. 2017;28:2826–8.
17. Lian L, Zhang S, Yu Z, et al. The dietary freeze-dried fruit powder of Actinidia arguta ameliorates dextran sulphate sodium-induced ulcerative colitis in mice by inhibiting the activation of MAPKs. Food Funct. 2019;10:5768–78. https://doi.org/10.1039/c9fo00664h.
18. Yang J, Cheng M, Gu B, et al. CircRNA_09505 aggravates inflammation and joint damage in collagen-induced arthritis mice via miR-6089/AKT1/NF-κB axis. Cell Death Dis. 2020;11:833. https://doi.org/10.1038/s41419-020-03038-z.
19. Zhang C, Chen H, He Q, et al. Fibrinogen/AKT/Microfilament Axis promotes colitis by enhancing vascular permeability. Cell Mol Gastroenterol Hepatol. 2021;11:683–96. https://doi.org/10.1016/j.jcmgh.2020.10.007.

20. McCole DF, Rogler G, Varki N, et al. Epidermal growth factor partially restores colonic ion transport responses in mouse models of chronic colitis. Gastroenterology. 2005;129:591–608. https://doi.org/10.1016/j.gastro.2005.06.004.

Publisher's note